

**REMOVAL OF ACID ORANGE 7 IN MOVING
BED BIOFILM REACTOR (MBBR) WITH
POLYHYDROXYALKANOATE (PHA) PELLETS
AS THE BIOFILM CARRIER**

CHANG JIA YUN

UNIVERSITI SAINS MALAYSIA

2023

**REMOVAL OF ACID ORANGE 7 IN MOVING
BED BIOFILM REACTOR (MBBR) WITH
POLYHYDROXYALKANOATE (PHA) PELLETS
AS THE BIOFILM CARRIER**

by

CHANG JIA YUN

**Thesis submitted in fulfilment of the requirements
for the degree of
Master of Science**

June 2023

ACKNOWLEDGEMENTS

It is a humbling experience to acknowledge those people who have, mostly out of kindness, helped along the journey of my master's degree. I am indebted to so many for encouragement and support.

First and foremost, I would like to express my sincere gratitude to my research supervisor Dr. Ng Si Ling and co-supervisor Professor Dr. K Sudesh Kumar A/L C Kanapathi Pillai for their continuous assistance and dedicated involvement in every step throughout the process. Without their patience guidance, motivation and immense knowledge, this study would have never been accomplished.

My sincerest thanks are extended to the financial support from the Ministry of Higher Education Malaysia under Fundamental Research Grant Scheme with project code FRGS/1/2018/STG01/USM/02/16 to complete this project. I would also like to show gratitude to academic and technical officers of Universiti Sains Malaysia from School of Chemical Sciences, School of Biological Sciences, School of Physics, Centre for Global Archaeological Research, and Institute for Research in Molecular Medicine. They are my most respected Dr. Oh Wen Da, Dr. Ng Eng Poh, Dr. Ahmad Faiz Abdul Latip, Dr. Manoj Kumar Lakshman, Ms. Ang Shaik Ling, Mr. Yushamdan Yusof, Mr. Muhammad Ikhwan Harun and Mdm. Nor Dyna Zakaria for knowledge sharing of data interpretation, deduction, collection, and analysis.

I am very grateful to all those who have given me their friendship, put up with my odd hours, and provided me with lifts and practical helps during the preparation of my project. Especially great thanks to Dr. Yow Chuen Jye, Dr. Ngoh Ying Shin, Mr. Choong Zheng Yi, Mr. Billy Neoh Soon Zher, Mr. Ahmad Syauqi Taufiq, Mr. Tong Wei Sherng, Mr. Ma Yik Ken, Ms. Ng Wen Yih, Ms. Tang Hui Jia, and Ms. Wan Jia Hui.

TABLE OF CONTENTS

ACKNOWLEDGMENTS.....	ii
TABLE OF CONTENTS.....	iii
LIST OF TABLES.....	vii
LIST OF FIGURES.....	ix
LIST OF SYMBOLS.....	xiv
LIST OF ABBREVIATIONS.....	xvi
LIST OF NOMENCLATURE.....	xviii
ABSTRAK.....	xix
ABSTRACT.....	xxi
CHAPTER 1 INTRODUCTION.....	1
1.1 Background of study.....	1
1.2 Problem statements.....	5
1.3 Research objectives.....	7
1.4 Scope of study.....	7
1.5 Overview of thesis.....	8
CHAPTER 2 LITERATURE REVIEW.....	11
2.1 Azo dyes and acid orange 7 (AO7).....	11
2.1.1 Sources and effects.....	12
2.2 Biological treatment of azo dyes.....	13
2.2.1 Azo dyes biodegradation mechanism.....	13
2.2.2 Sequencing batch reactor (SBR).....	14
2.3 Moving bed biofilm reactor (MBBR) system.....	16
2.4 Important characteristics of a biofilm carrier.....	19
2.4.1 Surface hydrophilicity.....	19
2.4.2 Surface roughness.....	21
2.4.3 Shape and surface area.....	21
2.5 Polyhydroxyalkanoate (PHA) as a potential biofilm carrier.....	22
2.5.1 Importance of PHA characterization.....	24
2.6 Biofilm development stages.....	25
2.6.1 Formation of anaerobic layer in biofilm.....	28

2.7	Factors affecting the MBBR performances.....	29
2.7.1	Activated sludge (AS) concentration.....	29
2.7.2	Organic substrate loading concentration.....	31
2.7.3	Acclimatization process.....	32
2.8	Response surface methodology (RSM).....	32
2.8.1	Design of experiment (DOE).....	33
2.8.2	Application of central composite rotatable design (CCRD)...	34
2.8.3	Statistical analysis.....	35
2.9	Kinetic modelling.....	35
2.10	Conclusion of literature review.....	37
	CHAPTER 3 MATERIALS AND METHODOLOGY.....	38
3.1	Flow chart of overall experiment.....	38
3.2	Characterization of PHA raw material.....	39
3.2.1	Gas chromatography (GC) analysis.....	39
3.2.2	Fourier transform infrared spectroscopy (FTIR) analysis.....	40
3.2.3	Thermal gravimetric analysis (TGA).....	40
3.2.4	Differential scanning calorimetry (DSC) analysis.....	40
3.3	Preparation and characterization of PHA biofilm carrier.....	41
3.3.1	Water contact angle (WCA) analysis.....	41
3.3.2	Scanning electron microscopy (SEM) analysis.....	42
3.3.3	Atomic force microscopy (AFM) analysis.....	42
3.3.4	Auto-titration zeta potential analysis.....	43
3.4	Set up and operation of reactor for biofilm development.....	43
3.4.1	Monitoring of reactor condition prior inoculation of PHA biofilm carrier.....	44
3.5	Investigation on the biofilm development on PHA biofilm carrier....	45
3.5.1	Determination of biofilm thickness.....	46
3.5.2	Extraction of extracellular polymeric substances (EPS).....	46
3.5.2(a)	Polysaccharides (PS) determination.....	47
3.5.2(b)	Protein (PN) determination.....	47
3.6	Batch studies of AO7 decolourization.....	48
3.6.1	Preliminary studies: One-factor-at-a-time (OFAT) studies....	48

3.6.2	Kinetics determination of AO7 decolourization.....	49
3.6.3	Response surface methodology (RSM): Design of experiment (DOE).....	49
3.6.4	Experimental set up.....	51
3.6.5	Statistical analysis and validation test.....	51
3.7	Isolation of AO7 decolourizing microorganism.....	51
3.7.1	Preparation of nutrient rich (NR) media and agar.....	51
3.7.2	Isolation of microorganism from mature biofilm.....	52
3.7.3	Determination of AO7 decolourization ability of microbial strain.....	52
3.8	Identification of AO7 decolourizing microorganism.....	53
3.8.1	Gram staining.....	53
3.8.2	Extraction of genomic deoxyribonucleic acid (gDNA).....	54
3.8.3	Amplification of 16S rRNA gene.....	55
3.8.4	Agarose gel electrophoresis.....	56
3.8.5	Identification and phylogenetic analysis of 16S rRNA gene...	57
CHAPTER 4 RESULTS AND DISCUSSION.....		58
4.1	Characterization of PHA raw materials.....	58
4.1.1	GC analysis.....	58
4.1.2	FTIR analysis.....	59
4.1.3	TGA.....	60
4.1.4	DSC analysis.....	61
4.2	Characterization of PHA biofilm carrier.....	62
4.2.1	SEM analysis.....	62
4.2.2	WCA analysis.....	65
4.2.3	Auto-titration zeta potential analysis.....	66
4.3	Monitoring of reactor condition prior inoculation of PHA biofilm carrier.....	67
4.4	Physicochemical analyses of biofilm at different development phases.....	68
4.4.1	Determination of biofilm thickness.....	68
4.4.2	AFM analysis.....	71

4.4.3	SEM analysis.....	74
4.4.4	Determination of PS and PN.....	74
4.5	Batch studies of AO7 decolourization.....	77
4.5.1	Preliminary studies: OFAT studies.....	77
	4.5.1(a) Effects of suspended sludge and initial AO7 concentration.....	77
	4.5.1(b) Effects of PHA pellet packing volume in MBBR.....	79
4.5.2	Kinetics of AO7 decolourization.....	80
4.5.3	RSM: Statistical optimization of AO7 decolourization	81
	4.5.3(a) Development and analysis of regression models.....	81
	4.5.3(b) Evaluation of the factors influencing the AO7 decolourization.....	87
	4.5.3(c) Interaction effects of operational factors on the AO7 decolourization.....	88
	4.5.3(d) Response surface optimization and validation.....	93
4.6	Isolation of AO7 decolourizing microorganism.....	96
4.7	Identification of AO7 decolourizing microorganism.....	99
	CHAPTER 5 CONCLUSION AND FURTUE RECOMMENDATIONS	106
5.1	Conclusion.....	106
5.2	Recommendations for future research.....	108
	REFERENCES.....	109
	APPENDICES	
	LIST OF PUBLICATIONS	

LIST OF TABLES

		Page
Table 2.1	Classification of azo dyes in colour index system.....	12
Table 2.2	Chemical structure and characteristic of AO7.....	12
Table 3.1	Tabulation of chapter, section, and sub section in APHA standard methods for the testing parameters applied in reactor monitoring	45
Table 3.2	Experiment complete design matrix with coded factors of CCRD.....	50
Table 3.3	Coded and actual values of process parameters in CCRD	50
Table 4.1	GC analysis data of PHA granules.....	58
Table 4.2	R^2 value of the kinetic models fitting for AO7 decolourization.....	80
Table 4.3	Experiment complete design matrix with coded factors of CCRD.....	82
Table 4.4	ANOVA for response surface reduced quadratic model for AO7 decolourization efficiency.....	83
Table 4.5	ANOVA for response surface reduced quadratic model for AO7 decolourization rate constant.....	84
Table 4.6	Assessment of DNA concentration and purity of the extracted gDNA from microbial colony and the amplified rRNA that encoded in gDNA.....	101
Table 4.7	Microbial rRNA gene identification of the microbial isolates, with the top hits of the rRNA BLAST results in the database of NCBI GenBank.....	101

Table 4.8	Microbial species and decolourization ability of azo dyes...	105
Table A1	The time course raw data of AO7 decolourization in OFAT experiments.....	131
Table A2	The time course raw data of the AO7 decolourization in RSM experiments.....	135

LIST OF FIGURES

		Page
Figure 2.1	Mechanisms for the (a) diazotization and (b) azo-coupling reactions.....	11
Figure 2.2	General overview of the fate of AO7 azo dye and colourless aromatic amines in biological treatment under anaerobic and aerobic condition.....	14
Figure 2.3	The formation of EPS linkages via hydrogen bonds between microbial cell walls and biofilm carriers with hydrophilic energy surface.....	20
Figure 2.4	The chemical structure of PHA molecular chain.....	22
Figure 2.5	Typical biofilm formation steps.....	25
Figure 2.6	The illustration of biofilm structure with layer classification.....	28
Figure 3.1	Flow chart of the five main parts involved in the experimental works in the study of AO7 decolourization in MBBR with PHA pellets as the biofilm carriers.....	38
Figure 3.2	Preparation of PHA pellets: (a) rat faecal granules, (b) powdered PHA, and (c) PHA pellets after hydraulic pressed.....	41
Figure 3.3	Schematic diagram of 1 L MBBR with PHA pellets as biofilm carrier.....	44
Figure 4.1	FTIR spectrum of PHA.....	60
Figure 4.2	TGA thermogram of PHA.....	61
Figure 4.3	DSC analysis of PHA.....	62
Figure 4.4	Disintegration of PHA pellet without thermal treatment after immersion into water.....	63

Figure 4.5	SEM images of (a) surface view and (b) cross section view for SEM analysis of PHA pellet treated thermally at different temperature.....	64
Figure 4.6	WCA analysis of PHA pellets treated with different temperatures.....	65
Figure 4.7	Zeta potential of PHA and AS as a function of pH.....	66
Figure 4.8	Performance analysis of AS throughout the AO7 acclimatization with results of (a) MLSS, (b) MLVSS, (c) SVI, and (d) effluent SS.....	68
Figure 4.9	Growth curves of biofilm in terms of (a) biomass weight and (b) biofilm thickness.....	69
Figure 4.10	(a) PHA pellets without porous design and (b) commercial high density polyethylene carriers with porous grid well design (arrow pointed).....	71
Figure 4.11	AFM images of biofilm surfaces at different growth stages	72
Figure 4.12	Plots of (a) MPH and RMS surface roughness and (b) skewness and kurtosis for biofilm growth.....	73
Figure 4.13	SEM imaging of PHA pellet (a) without biofilm and (b) with biofilm that formed by microbial colonization	74
Figure 4.14	Plots of (a) EPS, (b) PS and (c) PN content in the biofilm at different growth phase.....	76
Figure 4.15	OFAT analysis with response of AO7 decolourization efficiency by different (a) suspended sludge concentration and (b) initial AO7 concentration.....	78
Figure 4.16	OFAT analysis with response of AO7 decolourization efficiency by different PHA pellet packing volume.....	79

Figure 4.17	(a) Normal probability plot of the studentized residuals and (b) plot of studentized residuals versus predicted response values for (i) AO7 decolourization efficiency and (ii) AO7 decolourization rate constant.....	85
Figure 4.18	Plot of actual response value versus predicted response value of (a) AO7 decolourization efficiency and (b) AO7 decolourization rate constant.....	86
Figure 4.19	Effects of three independent factors in perturbation plots for response in (a) AO7 decolorization efficiency and (b) AO7 decolourization rate constant.....	86
Figure 4.20	(a) Interaction effects between suspended sludge concentration and initial AO7 concentration on (a) AO7 decolourization efficiency and (b) AO7 decolourization rate constant in (i) 3D response surface plots and (ii) 2D contour plots.....	89
Figure 4.21	Variation of median SOUR values of suspended sludge without acclimatization and with acclimatization to AO7 at 10 mg/L.....	90
Figure 4.22	Interaction effects between initial AO7 concentration and PHA pellet packing volume on (a) AO7 decolourization efficiency and (b) AO7 decolourization rate constant in (i) 3D response surface plots and (ii) 2D contour plots.....	91
Figure 4.23	Interaction effects between suspended sludge concentration and PHA pellet packing volume on (a) AO7 decolourization efficiency and (b) AO7 decolourization rate constant in (i) 3D response surface plots and (ii) 2D contour plots.....	94
Figure 4.24	Validation of response surface optimization design involving the interaction between variables.....	95

Figure 4.25	The biofilm microbial inoculum culture on NR plate at 30 °C with (a) dilution factor 10^2 up to 10^6 for 24 h, (b) with dilution factor 10^5 and 10^6 for 48 h and (c) with dilution factor 10^5 and 10^6 for 72 h.....	97
Figure 4.26	(a) Isolation of microbial strains with distinct morphology and (b) streak culture of the microbial strains on NR plates.	98
Figure 4.27	AO7 decolourization assessments for the isolated microbial strains, treating 5 mg/L, 20 mg/L, and 50 mg/L AO7, respectively.....	98
Figure 4.28	Gram staining assessment of the total 5 selected microbial strains that capable decolourize AO7.....	99
Figure 4.29	Feature of agarose gel electrophoresis showed Lane A1 was the gene ruler 1 kb Plus DNA ladder. Lane B1 to B5 were the unamplified gDNA with the band size at about 20000 bp, and Lane C1 to C5 were the amplified rRNA encoded in gDNA, where the band size of both 16S and ITS rRNA revealed at about 1500 bp and 600 bp, respectively. Unamplified gDNA of microbial 1, 2, 3, 4, and 5 were represented with Lane coded B1, B2, B3, B4, and B5, respectively, and the amplified rRNA encoded in gDNA of microbial 1, 2, 3, 4, and 5 were represented with Lane coded C1, C2, C3, C4, and C5.....	100
Figure 4.30	The neighbour-joining phylogenetic analysis of (a) bacterial category of <i>Leclercia sp.</i> strain USM.JY1S.LKQ, <i>Leuconostoc citreum</i> strain USM.JY2S.LKQ, <i>Leuconostoc citreum</i> strain USM.JY3S.LKQ, and <i>Bacillus cereus</i> strain USM.JY5S.LKQ and (b) fungal category of <i>Rhodotorula mucilaginosa</i> strain USM.JY4S.LKQ with its closely related taxa.....	102

Figure A1	Calibration curve of AO7 concentration.....	130
Figure A2	SOUR results for unacclimatized AS and acclimatized AS at 5 and 10 mg/L AO7.....	138
Figure A3	GPC analysis for the PHA pellet that introduced into the reactor over period up to 10.5 months.....	139
Figure A4	Evaluation of microbial consortium from biofilm at maturation phase on NR agar plate consisting with poly(3HB) and 11 % HHx.....	139

LIST OF SYMBOLS

bp	Base pair
L_f	Biofilm thickness
cm	Centimetre
R^2	Correlation Coefficient
cm^3	Cubic centimetre
Da	Dalton
$^{\circ}\text{C}$	Degree of Celsius
$^{\circ}\text{C}/\text{min}$	Degree of Celsius per minute
$^{\circ}$	Degrees
k_1	First-order rate constant
F	Fisher variation ratio
g	Gram
g/cm^3	Gram per cubic centimetre
g/L	Gram per liter
$\times g$	Gravitational force
h	Hour
pI	Isoelectric point
kb	Kilo base pairs
kV	Kilovolt
L	Liter
λ_{max}	Maximum absorbance wavelength
μL	Microliter
μm	Micrometer
μM	Micromolar
mg	Milligram
mg/h	Milligram per hour
mg/L	Milligram per liter
mg/mL	Milligram per milliliter
mL	Millilitre
mL/g	Millilitre per gram

mL/L	Millilitre per litre
mL/mg	Millilitre per milligram
mL/min	Millilitre per minute
mM	Millimolar
min	Minute
M	Molarity
M_w	Molecular weight
×	Multiplication sign
ng/ μ L	Nanogram per microlitre
nm	Nanometer
day ⁻¹	per day
h ⁻¹	per hour
%	Percentage
% (v/v)	Percentage in volume over volume
% (w/v)	Percentage in weight over volume
cm ⁻¹	Reciprocal wavelength
rpm	Revolutions per minute
k_2	Second-order rate constant
sp.	Species
V	Volt
vol%	Volume percentage
wt. %	Weight percentage
k_0	Zero-order rate constant

LIST OF ABBREVIATIONS

3HB	3-hydroxybutyrate
3HHx	3-hydroxyhexanoate
AO7	Acid orange 7
AS	Activated sludge
ANOVA	Analysis of variance
AFM	Atomic force microscopy
BLAST	Basic local alignment search tool
BSA	Bovine serum albumin
CME	Caprylic acid methyl ester
CER	Cation exchange resin
CCRD	Central composite rotatable design
COD	Chemical oxygen demand
CFU	Colony forming unit
DNA	Deoxyribonucleic acid
DOE	Design of experiment
DSC	Differential scanning calorimetry
DO	Dissolved oxygen
dsDNA	Double stranded DNA
EDTA	Ethylene-dinitrilo-tetraacetic acid
EPS	Extracellular polymeric substances
FTIR	Fourier transform infrared spectroscopy
GC	Gas chromatography
GPC	Gel permeation chromatography
gDNA	Genomic deoxyribonucleic acid
HPLC	High performance liquid chromatography
HRT	Hydraulic retention time
HHx	Hydroxyhexanoate
LB-EPS	Loosely-bound EPS
MLSS	Mixed liquor suspended solids
MLVSS	Mixed liquor volatile suspended solids

MEGA	Molecular evolutionary genetic analysis
MPH	Most probable height
MBBR	Moving bed biofilm reactor
NCBI	National Centre for Biotechnology Information
NR	Nutrient rich
OFAT	One-factor-at-a-time
PBS	Phosphate buffer solution
PHA	Polyhydroxyalkanoate
PCR	Polymerase chain reaction
PS	Polysaccharides
PN	Protein
RSM	Response surface methodology
rRNA	Ribosomal ribonucleic acid
RMS	Root mean square
SEM	Scanning electron microscopy
SBR	Sequencing batch reactor
SV ₃₀	Settle sludge volume
ssDNA	Single stranded DNA
SVI	Sludge volume index
SRT	Solid retention time
SS-EPS	Soluble-surface EPS
SOUR	Specific oxygen uptake rate
SS	Suspended solids
TGA	Thermal gravimetric analysis
3D	Three-dimensional
TB-EPS	Tightly-bound EPS
TAE	Tris-acetate-EDTA
2D	Two-dimensional
UV	Ultraviolet
UV-vis	Ultraviolet-visible
WCA	Water contact angle

LIST OF NOMENCLATURE

NH_4Cl	Ammonium chloride
$\text{CaCl}_2 \cdot 2\text{H}_2\text{O}$	Calcium chloride dihydrate
CuSO_4	Copper (II) sulphate
HCl	Hydrochloric acid
$\text{Cl}_3\text{Fe} \cdot 6\text{H}_2\text{O}$	Iron (III) chloride hexahydrate
$\text{MgSO}_4 \cdot 7\text{H}_2\text{O}$	Magnesium sulphate heptahydrate
NaH_2PO_4	Monosodium phosphate
KBr	Potassium bromide
KCl	Potassium chloride
KH_2PO_4	Potassium dihydrogen phosphate
NaHCO_3	Sodium bicarbonate
Na_2CO_3	Sodium carbonate
NaCl	Sodium chloride
NaOH	Sodium hydroxide
Na^+	Sodium ion
$\text{C}_4\text{H}_4\text{Na}_2\text{O}_6$	Sodium tartrate
SO_3^-	Sulfonate ion
Tris-Cl	Tris-chloride
Na_3PO_4	Trisodium phosphate
3HB	3-hydroxybutyrate

**PENYINGKIRAN ASID OREN 7 DALAM REAKTOR BIOFILEM KATIL
BERGERAK (MBBR) DENGAN PELET POLIHIDROKSIALKANOAT
(PHA) SEBAGAI PEMBAWA BIOFILEM**

ABSTRAK

Reaktor lapisan biologi bergerak menggunakan kedua-dua enapcemar teraktif terampai dan tidak bergerak untuk memulihkan air sisa. Pemilihan dan penggunaan bahan polimer hijau yang berkesan sebagai pembawa lapisan biologi boleh mengurangkan penghasilan sisa sekunder polimer tidak terurai. Penyelidikan ini bertujuan untuk menilai keberkesanan pelet polihidroksialkanoat (PHA) yang boleh biorosot sebagai pembawa lapisan biologi untuk merawat asid oren 7 (AO7). PHA yang digunakan dalam kajian ini dicirikan sebagai poli(3-hidroksibutilrat-co-3-hidroksiheksanoat) di mana dapat dibentuk ke bentuk pelet melalui tekanan hidraulik. Rawatan haba seterusnya pada 140 °C selama 1 jam menawarkan permukaan pelet PHA dimiliki dengan sudut sentuhan air pada 56.80 ° yang didapati mampu ditumbuhkan dengan lapisan biologi pada 236 µm dengan nisbah protein kepada polisakarida > 1 dalam reaktor yang disesuaikan dengan 10 mg/L AO7. Lapisan biologi pada pelet PHA telah ditumbuhkan melalui tiga fasa pertumbuhan utama iaitu fasa permulaan, penyatuan dan pematangan. Analisis mikroskopi daya atom menunjukkan kekasaran permukaan PHA meningkat daripada 53 nm (fasa permulaan) kepada 182 nm (fasa pematangan). Keputusan ini menunjukkan pertumbuhan lapisan biologi pada pelet PHA dengan sokongan daripada kejayaan pengimejan mikroskop elektron pengimbasan menangkap sel mikrob sfera dengan bahan polimer ekstraselular dalam lapisan biologi. Aktiviti penyelidikan dilanjutkan dengan metodologi

permukaan tindak balas untuk mengkaji kesan interaksi antara faktor kepekatan enapcemar terampai (1000 – 6000 mg/L), kepekatan awal AO7 (6 – 20 mg/L), dan isipadu pembungkusan pelet PHA (6 – 20 vol%) untuk kecekapan penyahwarnaan AO7 dan kinetik. Analisis menunjukkan bahawa kecekapan penyahwarnaan AO7 dipengaruhi dengan ketara oleh kepekatan enapcemar terampai dan isipadu pembungkusan pelet PHA dengan kinetik tertib pertama. Mengikut model kuadratik dengan kecukupan memuaskan dengan penentuan pekali 0.9532 dan 0.8647, masing-masing bagi ramalan kecekapan penyahwarnaan AO7 dan pemalar kadar, keadaan optimum untuk penyahwarnaan AO7 telah disahkan pada 5100 mg/L kepekatan enapcemar terampai, 10 mg/L kepekatan awal AO7, dan 20 vol% isipadu pembungkusan pelet PHA. Kecekapan penyahwarnaan AO7 optimum ialah 96.44 % pada pemalar kadar 0.3550 h^{-1} . Keberkesanan penyahwarnaan didapati disumbangkan daripada mikrob yang dikenalpasti iaitu *Leclercia adecarboxylata*, *Leuconostoc citreum*, *Bacillus cereus*, dan *Rhodotorula mucilaginosa*.

REMOVAL OF ACID ORANGE 7 IN MOVING BED BIOFILM REACTOR (MBBR) WITH POLYHYDROXYALKANOATE (PHA) PELLETS AS THE BIOFILM CARRIER

ABSTRACT

Moving bed biofilm reactor utilizes both suspended and immobilized activated sludge to remediate wastewater. Selection and application of effective green materials as the biofilm carrier could reduce the production of secondary non-degradable polymer waste. This research aimed to assess the efficacy of biodegradable polyhydroxyalkanoate (PHA) pellets as the biofilm carrier to treat acid orange 7 (AO7). The PHA used in this research was characterized as poly(3-hydroxybutyrate-co-3-hydroxyhexanoate) where successfully shaped into pellet form through hydraulic pressed. Subsequent thermal treatment at 140 °C for 1 h offered the surface of PHA pellet possessed with water contact angle at 56.80 ° which found to capable developed with 236 µm biofilm with protein to polysaccharides ratio > 1 in reactor that acclimatized to 10 mg/L AO7. The biofilm on the PHA pellets were developed through three major growth phases which were initial, consolidation and maturation phases. Atomic force microscopy analysis showed the PHA surface roughness increased from 53 nm (initial phase) to 182 nm (maturation phase). These results indicated the growth of biofilm on the PHA pellets with the support from scanning electron microscopy imaging success captured the spherical microbial cells embedded in the extracellular polymeric substances of the biofilm. The research activity was extended with response surface methodology to examine the interaction effects among factors of suspended sludge concentration (1000 – 6000 mg/L), initial AO7 concentration (6 – 20 mg/L), and PHA pellet packing volume (6 – 20 vol%) for AO7 decolourization efficiency and kinetics. The analysis showed that the AO7 decolourization efficiency was

significantly affected by the suspended sludge concentration and the PHA pellet packing volume with first-order kinetics. According to the reduced quadratic models with satisfactory adequacy of 0.9532 and 0.8647 in coefficient determination for the predictions of AO7 decolourization efficiency and rate constant, respectively, the optimum conditions for AO7 decolourization was validated to be at 5100 mg/L suspended sludge concentration, 10 mg/L initial AO7 concentration, and 20 vol% PHA pellet packing volume. The optimum AO7 decolourization efficiency was 96.44 % at rate constant of 0.3550 h⁻¹. The decolourization effectiveness was found to be contributed from the identified microbial strains which were *Leclercia adecarboxylata*, *Leuconostoc citreum*, *Bacillus cereus*, and *Rhodotorula mucilaginosa*.

CHAPTER 1

INTRODUCTION

1.1 Background study

In this era of scientific and technological advancement, the world is currently experiencing scarcity of clean water owing from water pollution. Azo dyes are one of the major pollutants found in the wastewater from the textile industry and other manufacturing sectors, including paper, cosmetics, food, pharmaceutical and leather [1]. In this study, acid orange 7 (AO7) was chosen as the model organic pollutant because azo dye is the largest group of colourants used in textile industries (60 – 70 %) [2]. Discharge of wastewater containing dye into receiving waters is posing a threat to the aquatic ecosystem and human attributed to the toxicity and carcinogenicity of the dyes [3]. Therefore, it is important to adequately treat the wastewater containing dyes to avoid negative impacts on the environment and water resources. Biological treatments provide certain benefits over physicochemical processes like adsorption, ozonation, oxidation, and photodegradation. The advantages include well-understood treatment technology, enhanced organic content removal efficiency, economic effectiveness, and environmental friendliness [4].

Activated sludge (AS) consists of the mixed microorganism was reported to be able to decolourize AO7 [2, 5]. However, the AO7 decolourization performance could be affected by the high initial AO7 concentration due to the toxicity effect [6]. The limitations of the AS process can be overcome by applying moving bed biofilm reactor (MBBR) system. MBBR is an advanced AS process [7] by integrating suspended sludge and biofilm process [8]. MBBR is an efficient biological treatment system for treating wastewater in which biofilm carriers were introduced as substratum for the attachment of microbial cells for the formation of biofilm [8]. The advantages of

MBBR that incorporating biofilm process in achieving stable and enhanced removal efficiency have been extensively reported [7, 9]. The accumulation of AS on the carriers in MBBR system provides an additional AS inventory which could resulting in shorter hydraulic retention time (HRT) for organic pollutant degradation in wastewater [10]. Furthermore, with the addition of biofilm carriers in a MBBR, the formation of biofilm on the carrier medium was believed to allow the creation of anaerobic microbial zone in the inner layer of the biofilm. The stack up of microbial cells in the anaerobic layer of the biofilm is beneficial in promoting the anoxic decolourization process of azo dyes [11].

With regards to the biofilm carrier, the conventional inorganic material-based carriers were shown to have several disadvantages, such as slow biofilm formation, poor permeability, high flow resistance, and simple clogging [12]. The examples of inorganic material are activated carbon, zeolite, and ceramic [12]. To address the issues of inorganic material-based carriers, different inert organic-based materials were investigated and employed as the biofilm carriers [13]. The examples are polypropylene [14 – 15], polyethylene [16 – 19], polystyrene [20 – 21], and polyurethane [22 – 27]. However, these materials are still disadvantageous in creating the secondary microplastic wastes after used in wastewater treatment. Therefore, it came to the needs to explore alternative green biofilm carrier with the 100 % organic characteristic to benefit the environment without generating any microplastic wastes in the treatment systems, while also supplying the microbial environment with extra carbon source and electron donor for the promotion of biofilm growth.

In this study, the potential of polyhydroxyalkanoate (PHA) as a green biofilm carrier in MBBR were investigated. PHA are polyesters that bio-derived in nature through bacterial fermentation of sugars. It consists of building blocks of

hydroxyalkanoate with containment of methyl group in its chemical structure, where providing the thermoplastic properties [28]. In comparison with conventional petroleum-based polymers, the production of the biologically recovered native PHA is relatively greener as there is no extensive use of solvents and strong chemicals [28]. The characteristic of PHA that are biodegradable make PHA an eco-friendly biopolymer and do not possess secondary pollution problems [29]. Coupled with other properties of thermos-processible, non-toxic, and biocompatible, it allows different application of PHA in industries such as in drug delivery, food additives and medical implants [30]. In view of the biodegradability and biocompatibility of PHA, it can be explored as an alternative to replacing conventional biofilm carrier in biofilm process. To date, the report on using PHA as the biofilm carrier is sparse. In a study conducted by Muhd Aidil, *et al.* (2020) [31], PHA granules were successfully employed as biofilm carrier in MBBR treating phenol. The addition of PHA in the reactor was found to increase the biodegradation rates of phenol and chemical oxygen demand (COD). Nonetheless, further investigation on the characteristics of PHA and the effects of operational parameters would be vital in exploiting the potential of PHA as biofilm carrier. It was reported that PHA has similar hydrolytic resistance qualities to inorganic and inert organic-based biofilm carriers, and its unique natural hydrophilic surface is thought to increase the bio-affinity and adherence of microbial cells [29, 32].

The dynamicity of the dominating microbial colonization in a biofilm was greatly influenced by the properties of the carrier materials [33]. The surface properties of the carriers, such as surface roughness, zeta potential and wettability, have significant consequences on the microbial colonization [34]. Based on the research conducted by several researchers, the microbial immobilization is favourable on the carriers with the characteristics of high surface roughness [12], positive surface charge

[35], and high surface hydrophilic [36]. All these characteristics could facilitate the initial microbial cells attachment and the subsequent evolution into thicker biofilm. Hence, it is important to characterize the PHA pellets used in this study and to investigate its feasibility to be employed as a biofilm carrier.

The built-up of the biofilm started from the synthesis of extracellular polymeric substances (EPS) by microbial cells for colonization [8]. The stack up of the microbial cells during the biofilm formation occurs through several stages: starting from the initial attachment of cells onto the substratum surfaces, followed by the consolidation of microbial with EPS secretion, and lastly the maturation of microbial consortium with stable adhesion forces on the substratum. The initial attachment happened when the unicellular microorganisms deposited on the substratum to form a group matrix of biofilm [37]. The microbial adherence to the substratum was facilitated by the EPS which acts as slime to aggregate the microbial cells [38]. The main constituents of EPS are the polysaccharides (PS) and protein (PN) with high molecular weights (M_w) which promote the immobilization of microbial cells in biofilms and keep them in proximity structures [39].

Furthermore, it's important to conduct microbial identification in the biofilm to recognize the effective microbial strains that contribute to the degradation of organic pollutants. The findings are essential to document the potential microbial species and used as the references for future research and industrial applications in the sector of wastewater treatment. The anaerobic decolourizations of azo dyes by various effective microbial strains have been well researched. The examples of effective microbial strains that were able to contribute to azo bonds reduction are *Bacillus* sp. [40 – 41], *Aeromonas* sp. [42 – 43], *Pseudomonas* sp. [44 – 45], *Proteus* sp. [46], and *Enterococcus* sp. [47]. In this study, the key physicochemical characteristics of biofilm

on PHA throughout the biofilm development in MBBR treating AO7 and its microbial community were evaluated.

Last but not least, the optimization of the MBBR operational conditions is vital to achieve efficient dyes decolourization. The performance of a MBBR is affected by the operational parameters such as dye initial concentration, ratio of attached-growth to suspended-growth AS and the thickness of biofilm [7]. According to the literatures, the efficiency of micropollutant removal was highly reflected from the distinct specific microbial growth between attached-growth and suspended-growth AS [48]. In addition, the increase of biofilm thickness could promote the AO7 decolourization with improved first-order kinetic [49 – 50]. Nevertheless, the effects of these factors were studied individually and the information on the interaction effects on the efficacy of the system for dye decolourization is still limited. Hence, in this study, response surface methodology (RSM) was employed to investigate the interaction effects of the factors affecting the efficiency and kinetics of dye decolourization. The findings would provide understanding of the basis for optimizing MBBR set up in future research.

1.2 Problem statements

In the existing studies of MBBR systems, inorganic and inert organic material-based carriers were commonly applied for biofilm development and the subsequent bioremediation in wastewater [12, 34]. However, these materials are still detrimental in terms of producing secondary wastes after being utilized in wastewater treatment. Nonetheless, the exploration on the capability of biodegradable organic material-based carriers as biofilm carrier in MBBR system is still lacking. Hence, to establish a greener biofilm carrier to minimize the production of secondary wastes, PHA, a biopolymer with reported 100 % biodegradable property, was selected as novel biofilm

carrier in this research work. With the sparse of PHA application in MBBR, a detailed investigation on the PHA characteristics is needed. The first concern is the thermal transition characteristics of PHA which consequently decide the feasibility of PHA to be converted into reliable biofilm carrier. The second challenge is the effectiveness of PHA to serve as a substratum for biofilm development. Thus, the surface properties of the PHA carrier are the important input to be explored for further understanding on the interactions between PHA and microbial cells. Furthermore, it is of great interest to evaluate the biodegrading ability of biofilm developed on the PHA carrier for bioremediation. In this study, AO7 as the widely used azo dyes in textile industries was being selected as the model pollutant in the assessment of the efficacy of biofilm and MBBR for AO7 decolourization [2]. It is critical to fully comprehend the foundation for improving the MBBR setup by investigating the interaction effects of the influencing factors that impact dye decolourization efficiency and kinetics. The impacts of influencing factors were explored singly at a time in most previous research, which further limited reliable information on the interaction effects on the efficacy of the MBBR system for dye decolourization [7]. As a result, RSM has the advantage of optimizing the analytical process using multivariate statistical information and identifying the most significant influencing factor [51]. Microbial identification in the biofilm is also essential to determine the effective microbial strains that contribute to AO7 decolourization. The findings are critical for documenting prospective microbial species and could be utilized as references for future studies and industrial applications in the wastewater treatment systems.

1.3 Research objectives

This study aimed to investigate the efficacy of a MBBR system with PHA pellets as the biofilm carrier for AO7 decolourization. This study has five specific objectives as per listed below:

- i. To prepare and characterize PHA pellets for employment as biofilm carrier.
- ii. To investigate the biofilm development on PHA pellets in different growth phases.
- iii. To evaluate the interaction effects of physiochemical factors (dye initial concentration and biofilm carrier packing volume) and biological factors (suspended- and attached-growth sludge concentration) on the efficiency and kinetics of AO7 decolourization.
- iv. To optimize the AO7 decolourization in MBBR with PHA pellets as biofilm carrier.
- v. To identify the type of microbial community in the biofilm on PHA pellets.

1.4 Scope of study

This study was divided into four main parts. The first part was the preparation and characterization of PHA pellets which were used as the novel biofilm carrier in MBBR treating AO7. Hydraulic press methodology was established to prepare the PHA pellets. Thermal treatment was conducted to increase the mechanical stability of PHA pellets. The optimum treatment temperature was selected based on analyses of water contact angle (WCA) with the support of imaging view from scanning electron microscopy (SEM). The research work was then extended to the investigation on the development of biofilm on the PHA pellets in the MBBR. Characterization of biofilm was conducted, and the analyses include biofilm thickness determination, optical

microscopy analysis and glycoprotein content determination to evaluate both physicochemical and biological properties of the biofilm. The third part of the research work was to investigate the effects of physicochemical and biological factors, namely the suspended sludge concentration, initial AO7 concentration, and PHA pellet packing volume on the performance of MBBR in AO7 decolourization. Modelling and optimization of the operational factors were conducted using RSM. The last part of the study was the microbial identification in the biofilm that developed on the PHA pellets. Microorganisms that were capable to decolourize the AO7 were identified using techniques of microbial 16S rRNA genetic extraction, amplification, and sequencing.

1.5 Overview of thesis

This thesis consists of five chapters, comprising the details of research background, methodology, and research findings of the project.

In Chapter 1, MBBR was being introduced as an efficient biological treatment system for azo dye removal by using integrated suspended- and attached-growth AS. The disadvantages of conventional inorganic and inert organic material-based carriers were highlighted. PHA with biodegradable properties was introduced as the potential green biofilm carrier. The significance to study the interaction effects of factors influencing the MBBR performance and subsequently the optimization process was also highlighted. Besides that, the importance of the study of biofilm development and microbial identification was recognized to determine the effective microbial strains that contribute to pollutant removal.

Chapter 2 is a comprehensive literature review, which elaborates the chemistry of azo dyes and the microbial decolourization of azo dyes. The immobilized microbial technology in moving bed biofilm process was discussed by relating to the AS system

as the potential microbial source. The important characteristics of a biofilm carrier was being discussed such as the consideration of surface hydrophilicity, surface roughness, and surface area to relate the potential of PHA to equipped with the reliable advantages as biodegradable biofilm carrier. Also, the four biofilm development stages being discussed are the microbial cells initial attachment, young biofilm formation, biofilm accumulation, and biofilm maturation. Besides that, the discussion included the influencing factors that affected the MBBR performance. The critical factors such as AS concentration, organic substrate loading concentration, and acclimatization process were being discussed. Lastly, the significance of RSM for the investigation of the interaction effects between the influencing factors was discussed.

Chapter 3 focuses on the methodology to characterize the PHA raw material and followed by the preparation of PHA pellets as biofilm carrier by using hydraulic press method, which is in line with objective (i). The mechanical stability PHA pellets was further analysed using the important techniques of WCA and SEM. Methodology to analyse the developed biofilm that relates to objective (ii) was being discussed. The analyses involved the optical microscopy, gravimetric biofilm thickness determination, and glycoprotein content determination in EPS. To meet objectives (iii) and (iv), design of experiment (DOE) using central composite rotatable design (CCRD) was used to study the interaction effects among the factors of suspended sludge concentration, initial AO7 concentration, and PHA pellet packing volume. Lastly, to achieve objective (v), microbial community identification in the biofilm on PHA pellets was conducted using techniques of microbial 16S rRNA genetic extraction, amplification, and sequencing.

In Chapter 4, the potential of PHA for application as biofilm carrier in MBBR was explored. The findings showed the feasibility of thermally treated PHA to serve

as a biofilm carrier for the attachment of suspended AS and subsequently biofilm development. The findings were associated to objective (i). The attached growth biofilms showed its functionality to decolourize the AO7 after the maturation biofilm development. The insights of the biofilm development that relate to the objective (ii) were being evaluated based on the results from optical scanning microscopy integrated with the biochemical determination. Besides that, in line with objective (iii), the interaction effects of MBBR operational factors (suspended sludge concentration, initial AO7 concentration, and PHA pellet packing volume) on the AO7 decolourization efficiency and kinetics were analysed. The objective (iv) was achieved through conduction of RSM with CCRD to optimize the operational conditions for integrated biofilm-suspended biodegradation process for AO7 decolourization. Finally, the microbial community in biofilm with AO7 decolourizing ability were successfully identified and the findings catch sight of the objective (v).

In Chapter 5, the overall research findings were concluded with the recommendation of future work to further modify the carrier shape and structure of PHA biofilm carrier. The successful biofilm growth on the PHA convinced the worth of further exploration to commercialize the PHA-based carrier that able meet the requirement of wastewater treatment industry.

CHAPTER 2

LITERATURE REVIEW

2.1 Azo dyes and acid orange 7 (AO7)

Azo dyes have been widely explored commercially in the development of cost-effective synthetic colorant through simple diazotization of primary aromatic amine, followed by azo coupling of diazonium salt (Fig. 2.1) [52 – 54]. The azo dyes are characterized by the functional azo group of $-N=N-$ in uniting two groups of alkyls and/or aryls symmetrically and/or asymmetrically [52]. Table 2.1 provides the colour index number classifying the series of synthesized azo dyes based on the respective azo group [52, 55]. Meanwhile, the synthesized azo dyes can be further categorized into three major properties group, according to their nature charge which are anionic reactive dyes, cationic basic dyes and non-ionic disperse dyes [56]. Among the mentioned azo properties group, the anionic azo dyes are the dyes that strongly soluble in water with the presence of sulfonate (SO_3^-) reactive group and this characteristic makes the anionic dyes extensively applied in dye industry [57]. The most used anionic dye in dye industry is AO7 which cover more than 15 % of the worldwide dye production in the textile industry [58]. Table 2.2 shows the chemical structure and characteristic of AO7, a mono azo dye with organic properties, which was selected as the model pollutant in this study.

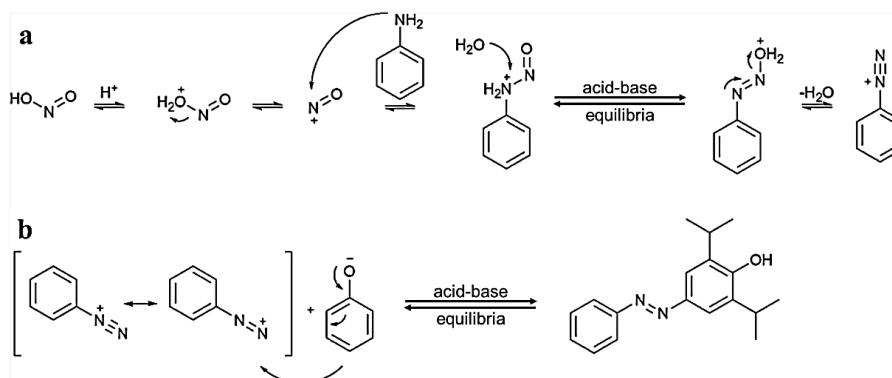
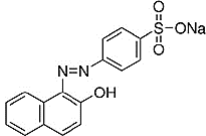


Figure 2.1: Mechanisms for the (a) diazotization and (b) azo-coupling reactions [53].

Table 2.1: Classification of azo dyes in colour index system [52, 55].

Azo group classification	Colour index number
Mono azo dyes	11000 – 19999
Bis azo dyes	20000 – 29999
Tris azo dyes	30000 – 34999
Poly azo dyes	35000 – 36999
Azoic azo dyes	37000 – 39999

Table 2.2: Chemical structure and characteristic of AO7 [56].

Chemical structure	Colour index number	Maximum absorbance wavelength (λ_{max}), nm	M _w , g/mol
	15510	484	350.32

2.1.1 Sources and effects

The azo dyes present in wastewater majorly discharged from the textile industry and various manufacturing industry of paper, cosmetics, food, pharmaceutical, and leather. It was statistically reported that about 15 to 50 % of azo dyes were abandoned as wastewater after the processing of the highlighted products, especially in developing country due to relaxed environmental control regulation [1].

The release of carcinogenic aromatic amines as by-product of azo dyes degradation could cause the side effects of allergies, neurobehavioral impairment, neuroinflammatory stress, memory impairment and anxiogenic if after periods of bioaccumulation from unexpected incomplete treated wastewater [59].

Consequently, the European Commission has issued laws prohibiting the sales of the products of textile and leather that made with azo dyes with concentration exceeding 30 mg/L [1]. In view of the adverse effects resulting from the azo dyes, it is vital to remove the azo dyes before the industrial effluents are discharged into receiving waters.

2.2 Biological treatment of azo dyes

With regard to azo dyes removals, when compared to the physicochemical treatments such as adsorption, ozonation, oxidation, and photodegradation, the biological treatments have some advantages, including well-understood treatment technology, improved organic content removal efficiency, cost-effectiveness, and environmental friendliness [4].

2.2.1 Azo dyes biodegradation mechanism

Removal of azo dyes by degradation process involves the decolourization of azo dyes by cleavage of azo bond $-N=N-$. Fig. 2.2 illustrates the general reaction mechanism of azo dyes anaerobic decolourization and aerobic degradation in a biological treatment [60]. Complete removal of azo dyes in biological wastewater treatment system consists of two major processes. The first process involves the decolourization of azo dyes by reductive cleavage of azo bond $-N=N-$ under anaerobic condition. The following process is the aerobic degradation of the intermediate products of aromatic amines [61]. The colourless aromatic compounds are the sulphanic acid as sulphonated aromatic amines and 1-amino-2-naphthol compounds, where the chemical structures are illustrated in Fig. 2.2 [62]. Under aerobic conditions, the carcinogenic aromatic amines are mineralized via aromatic ring cleavage [63].

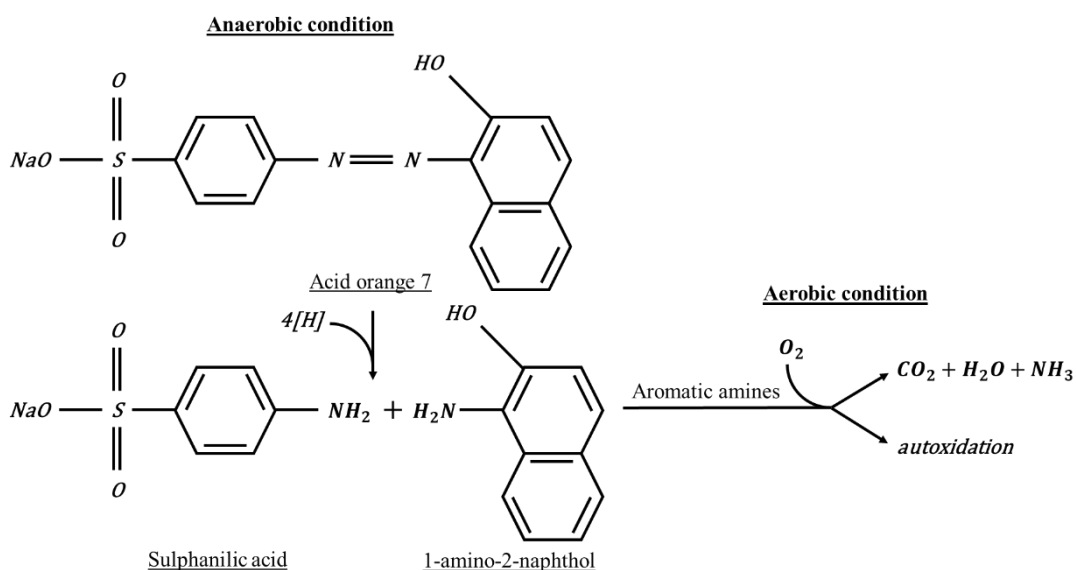


Figure 2.2: General overview of the fate of AO7 azo dye and colourless aromatic amines in biological treatment under anaerobic followed by aerobic condition [62].

2.2.2 Sequencing batch reactor (SBR)

The AS process is one of the biological treatments that removes organic matters from huge volume of wastewater in a relatively compact reactor [64]. The reactor set-up of a fill-and-draw AS system is referred as the sequencing batch reactor (SBR) [65]. In term of the appearance, AS is presented as bio-flocculated microbial aggregates with filamentous bulking behaviour [66 – 67]. SBR uses the AS to treat the organic matter through biologically mechanism as per discussed earlier (Section 2.2.1). AS composed of aerobic and anaerobic microbial cells which are capable to degrade organic compounds under appropriate designated microbial growth condition [68]. Widespread preference is given to the mixed microbial culture in the AS system for wastewater detoxification, including with the azo dyes degradation because it could provide a more effective rate of azo dye removal than the degradation approach only using individual microbial strain [63, 69].

The azo dye decolourization during the anaerobic phase in SBR was reported with colour removal efficiency up to 95 % [70]. The aerobic phase would only

contribute to decolourization if the remaining dye concentration after anaerobic phase is high resulted from the partial breakdown of azo dyes [70]. The best cycle time on bio-decolourization of azo dye in SBR achieving a high decolourization of > 90% was reported for the total cycle time of 24 h with the anaerobic-aerobic phase ratio at 1:1 [71]. In addition, it was noted that the bio-decolourization by the microbial cells in SBR usually followed the first-order kinetic expression [72]. However, different kinetic models still could be used to express the azo dye decolourization, depending on the molecular structures and enzymatic specialization of the microbial cells [73].

It was reported that the microbial enzymes secreted by the active microbial cells were the azo reductase and catechol 2,3-dioxygenase during anaerobic and aerobic phases, respectively [71]. There are a wide range of potential microbial cells that have been extensively explored in degrading azo dyes, including bacterial genus of *Pseudomonas*, *Escherichia*, *Rhodobacter*, *Enterococcus*, *Staphylococcus*, *Xenophilus*, *Corynebacterium*, *Clostridium*, *Micrococcus*, *Acinetobacter*, *Lactobacillus*, *Rhizobium*, *Proteus*, *Morganella*, *Aeromonas*, *Alcaligenes*, and *Klebsiella* [63]. These cultures could be found in the AS systems.

Although azo dyes removals using SBR systems were reported, the use of suspended AS in the conventional SBR systems was not under the optimized condition in view of its high sludge production and lack of active microbial cells in AS [12, 74]. This drawback could be resolved or improved by incorporating active microbial cells in the form of biofilm using MBBR system.

2.3 Moving bed biofilm reactor (MBBR) system

MBBR system refers to a system that utilized both suspended and immobilized AS to remediate wastewater. MBBR is an AS system added with free-floating substratum that give a vast surface area for colonization of microbial cells. The substratum is known as biofilm carrier. An effective carrier is the principal component in MBBR to facilitate the biofilm formation. The mixed microbial culture in the AS is the source of biofilm formation on the biofilm carrier, and the microbial community structures in the biofilm relies on the characteristic of the biofilm carrier [75 – 76].

In comparison to the SBR system, observable reduction in the inhibitory effects of toxic organic matter on the biochemical activities of the microbial cells was reported [77]. The MBBR systems are more appealing and promising in treating highly concentrated wastewater due to the substantial accumulation of microbial cells in the biofilm [78]. The accumulation of microbial cells on the substratum in MBBR provides an additional microbial inventory and thus a shorter HRT for organic pollutants degradation in wastewater [10]. The MBBR system's microbial residence duration was shown to be increased by immobilized microbial cells [79]. This increases the interaction between the target pollutant and the biofilm, which can significantly speed up the pollutant degradation [80]. In addition, it was reported that attached-growth AS exhibited greater resistance to the inhibitory effects of toxic organic chemicals compared to the suspended-growth system [81 – 82]. This is because the inner layer of biofilm experiences only minor exposure to inhibitory substrate compared to the outer layer. Thus, the overall solid retention time (SRT) of AS could be prolonged to remove the toxic organic chemicals via diffusion into the inner layer of biofilm [11].

Other advantages of MBBR include the reduced space requirements when compared to SBR, ease of upgrading existing facilities, low head loss when compared to submerged filter configurations, and fewer cleaning or backwash requirements [83].

Various inorganic and inert organic materials with hydrolytic resistance properties are widely used as biofilm carrier in MBBR system. It is discovered that the inorganic material-based biofilm carriers, with examples of activated carbon [84], zeolite [12] and ceramic [85] are pervasive and exhibit exceptional mechanical strength. Besides that, inorganic material-based carriers' rough surface and extensive porous structure could protect the microbial cells from shock loading while simultaneously offering a great habitat for biofilm adhesion [86]. In the study by Lim, *et al.* (2014) [84], activated carbon and zeolite were utilized as an adsorbent to absorb the AO7 dye molecules as well as a to serve as a support material for the biofilm adhesion. The deployed biofilm system achieved nearly complete AO7 decolourization and > 80 % COD elimination within 3 h of treatment time [84]. In another work by Amin, *et al.* (2022) [85], an anaerobic biodegradation using a small ceramic-supported graphene oxide membrane bioreactor was used for the removal of different dyes, such as AO7, reactive black 5 and direct blue 71 with mono-, di-, and tri-azo bonds, respectively. The results showed the attainment of maximum colour decolourizations at 99 %, 96 % and 92 % for AO7, reactive black 5, and direct blue 71, respectively.

On the other hand, inert organic material-based biofilm carriers, with examples of polypropylene [87 – 88], polyethylene [16 – 17, 89 – 90], polystyrene [91 – 92], and polyurethane [22 – 23, 25, 27, 93 – 94] showed their advantages of low density, stability, resistance to ageing and biodegradation, and great mechanical strength [95]. The efficacy of MBBR using inorganic or inert organic material-based carriers were

extensively studied. Sonwani, *et al.* (2021) [16] used polyethylene and polypropylene for the decolourization of Congo red azo dye. The MBBR packed with this low-density carrier was able to decolourize the Congo red dye up to 99.2 % at the loading concentration of 40 mg/L [16]. There are examples of carrier surface modification by blending the polyethylene and polyurethane with cationic polyacrylamides and N-methyl diethanolamine, respectively, to increase the surface charges while maintaining the hydrophilicity properties to improve the biofilm formation [27, 96]. It was reported that the modified carrier possessed 1.3 times higher of biofilm attachment than the common polyurethane foam which was preferable for organic pollutant removal [27].

Albeit the applications of different inorganic and inert organic materials as biofilm carrier were reported, in term of drawbacks, inorganic material-based carriers were found to cause sluggish biofilm development, poor permeability, high flow resistance, and easy clogging [12]. For inert organic material-based carriers, they were found to have poor specific surface area compared to inorganic material-based carriers [95]. In the aspect of biodegradability, both inorganic and inert organic materials were non- or partial-degradable, which indirectly possess the problem of secondary waste production after being used as biofilm carrier in MBBR [12, 95]. Therefore, efforts should be made to explore for better option of biofilm carriers that satisfy all the requirements for promoting the microbial adherence and development while also being biocompatible and biodegradable.

2.4 Important characteristics of a biofilm carrier

The choice of carrier type is a key factor in ensuring adequate attachment of microbial cells in forming biofilm on the substratum surface. The selection of carrier with material density that is closer to or lower than the water density is crucial to ensure the movement of carriers inside the MBBR [97]. Microbial adherence is strongly influenced by characteristics of a carrier, where the surface hydrophilicity, electrophilicity, roughness, and surface area play crucial roles in guiding microbial adhesion to form biofilm.

2.4.1 Surface hydrophilicity

It is well acknowledged that the microbial cells secrete EPS to facilitate the microbial immobilization during the biofilm formation [39]. EPS are organic polymers of microbial origin that responsible for attaching cells and other particulate materials together via cohesion and to the substratum through adhesion [98]. PN and PS are the main constituents of the EPS, which provides the microbial cell walls functional properties with hydroxyl group ($-OH$), carboxyl group ($-COOH$), aldehyde group ($-CHO$) and carbonyl group ($-C=O$) [12]. These functional groups with its negatively charged nature promote the creation of van der Waal forces when interact with the hydrophilic surface [12, 99]. Besides that, hydrogen bonds can be formed between the functional groups of hydrophilic surfaces of carrier and microbial cell wall (Fig. 2.3). Hydrogen bonds formation strengthen the energy surface for the microbial attachment on the biofilm carrier. In addition, the biomass attachment rates could be improved with the provision of carrier surfaces consisting of adequate cationic and hydrophilic properties [100]. Hence, selection of biofilm carrier with hydrophilic surface with

greater zeta potential degree would benefit the interactions between the microbial cell wall and the biofilm carrier through surface charge attraction [12].

The wettability test can be used to evaluate a biofilm carrier's surface hydrophilicity [100]. The measurement of the carrier surface's water contact angle can be used to quantify the wettability [101], in which a hydrophobic surface would exhibit a contact angle greater than 90 degrees [27]. The level of hydrophilicity increases with decreasing contact angle. Microbial cells and the carrier surface may repel one another in pure polymeric carriers with a narrow range of wettability. Thus, a carrier with hydrophilic surface is preferred to promise the biofilm adhesion and development.

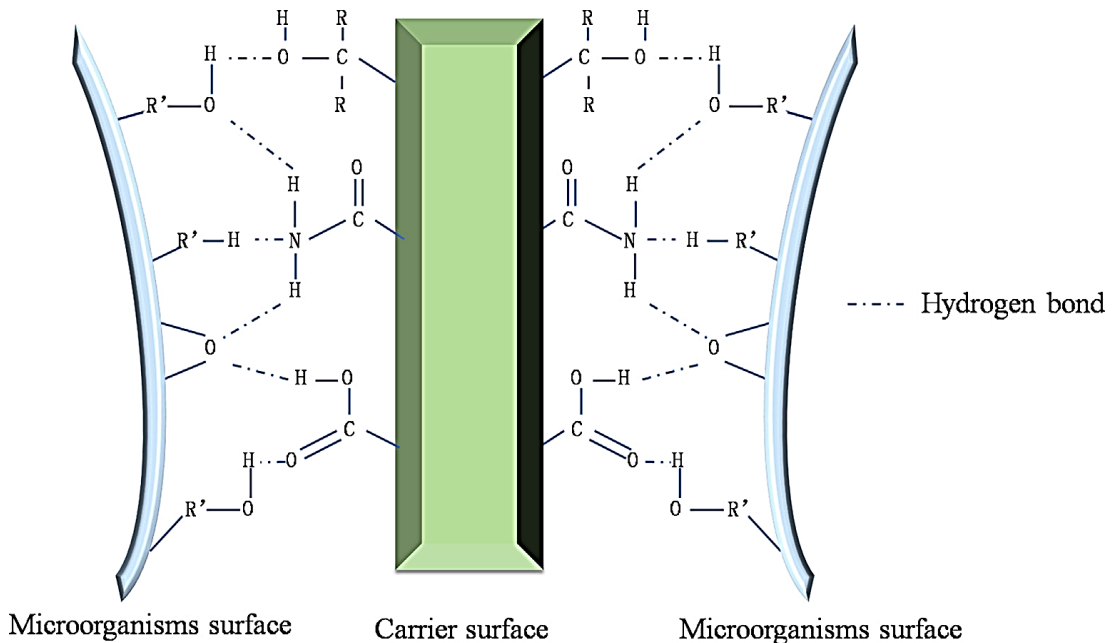


Figure 2.3: The formation of EPS linkages via hydrogen bonds between microbial cell walls and biofilm carriers with hydrophilic energy surface [12].

2.4.2 Surface roughness

A biofilm carrier's rough surface promotes rapid microbial growth and immobilization [100]. Surface roughness helps the microbial communities to form their first adhesion and to shield them from being ripped apart when biofilm carriers clash. Surface roughness of a carrier has a direct influence on the quantity of microbial cells attached, the rate of biofilm formation, and the texture of the biofilm. Jonstrup, *et al.* (2011) [102] reported that the Kaldnes carriers with smoother surface were more readily for microbial cells detachment if compared to Poraver carriers with rougher and porous surface. Furthermore, the anaerobic reactor with Poraver carriers displayed superior azo dyes removal than the reactor with Kaldnes carriers due to the variations in biofilm structure [102].

2.4.3 Shape and surface area

The bioremediation procedure in MBBR is reported to be directly impacted by the surface area of biofilm carriers [103]. The depth, diffusion, and thickness of a biofilm may be influenced by different carrier architectures. Besides that, the shearing strength and collision conditions of a carrier may be affected by the shape of the carrier. Various carriers in the shapes of disc [103], hollow duct cylinder [104], granular [105], sphere [106], flat pellet [107], star [108], fibrous [109], parabola [110], ellipsoidal [111], perfect cuboidal [112], spindle [113], O-ring [114], or spiral with hollow square [115], were employed, with the aim to maximise the surface area available for biofilm growth. The internal surface area of carriers can be increased for microbial adhesion by designing them with a cross structure [116]. Additionally, it has been shown that carriers with irregular shapes may shield biofilms from carrier collisions, liquid shear, and turbulence [117].

Also, the growth of the microbial cells can be expanded on the carriers with higher surface areas [118]. The specific surface areas of a biofilm carrier can be increased by converting the classical fixed sheet or layer forms of carrier into cubic or pellet form [118]. The increase in surface area also allows for greater microbial contact with nutrient medium provision which subsequently aids in promoting the microbial acclimatization and adaptation in MBBR [76].

2.5 Polyhydroxyalkanoate (PHA) as a potential biofilm carrier

PHA is a type of green polymer that possesses environmental benefits when compared to the conventional petroleum-based polymers. PHA are unique natural biopolyesters that are polymerized *in vivo* in microorganisms involving intracellular organic phospholipid or protein inclusions for energy storage within the cytoplasm cellular structure [29]. Fig. 2.4 shows the general structure of PHA [119]. From Fig 2.4, PHA are the organic bio-based polymeric materials that consist of bio-derived building blocks of hydroxyalkanoate ester groups. These molecular chains were synthesized naturally from the bacterial fermentation under the presence of excess carbon source and nutrient limitation [29, 120 – 121]. The biocompatible and non-toxic PHA has a wide range of uses in many different sectors, including the biomedical industry, which includes tissue engineering, bio-implant patches, medication delivery, surgery, and wound dressing [29].

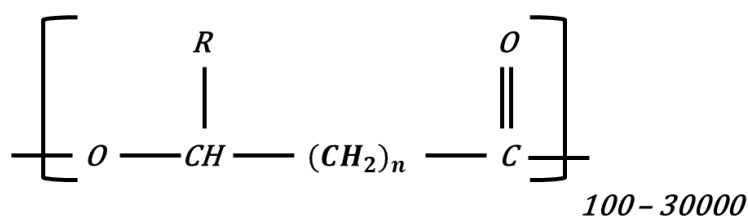


Figure 2.4: The chemical structure of PHA molecular chain [119].

As per discussed earlier, microbial adherence is strongly influenced by characteristics of a carrier, in which the surface hydrophilicity, electrophilicity, roughness, and surface area play crucial roles in guiding microbial adhesion to form biofilm. In comparison to the conventional carriers, the unique natural hydrophilic of PHA surface is believed to enhance the bio-affinity and adhesion of microbial EPS linkages [29, 32]. Besides that, PHA possesses similar hydrolytic resistance properties as inorganic and inert organic based biofilm carriers [29, 32], and it offers advantage of being biodegradable and thus can be explored as potential biofilm carriers to replace non-biodegradable inorganic and inert organic material-based carriers. Moreover, PHA has drawn more attention because of its slow-release properties [12]. Slow release is known as controlled release, in which PHA can be employed as biofilm carrier that capable provide nutrient source for biofilm at specific rate over a period while acting as solid substratum until its complete depletion or degradation by the microbial cells without generating any secondary waste [12]. Hence, it was believed that PHA carrier can provide at least two functions: as a biofilm carrier and as a solid-phase carbon source donor [12].

There are not many reports on application of PHA in wastewater treatment systems as of now. A brief evaluation of the use of PHA for denitrification in wastewater treatment was done by Hiraishi and Khan (2003) [122]. It was reported that the PHA functioned as solid matrices that favoured the growth of microbial films. In addition, PHA served as a consistent source of reducing power for denitrification. In a study by Muhd Aidil, *et al.* (2022) [31], the feasibility of PHA granules as biofilm carrier in the MBBR treating phenol was first explored. The biodegradation rates of phenol and the COD were observed to rise with the addition of PHA granules to the reactor. However, the mechanical stability of PHA required improvement in view of

the observed reduction in the packing volume of PHA after 128 days of use. Hence, further investigation on the properties of PHA biofilm carrier is necessary in exploiting the potential of PHA as a biofilm carrier.

2.5.1 Importance of PHA characterization

Characterization of PHA is essential prior to the preparation of biofilm carrier for MBBR application. The understanding of thermal properties of PHA was reported as important criteria to have upright thermal pre-treatment of PHA prior applied as biofilm carrier [31]. Native PHA possesses highly natural hydrophilic properties, hence a desirable thermal modification is necessary to control the level of surface wettability in order to avoid PHA dispersion while maintaining microbial attachment [29]. The importance of surface wettability of biofilm carrier is well described in Section 2.4.1. The thermal properties of PHA vary depending on the number of carbon side chains (methyl, ethyl, propyl, pentyl, or nonyl) in its chemical structure [119]. The melting point of PHA reduces with the increased of side chains or monomeric units, revealing a decrease in PHA crystallinity as well [123]. The most commonly employed methodology for the analysis of PHA thermal behaviour are the thermal gravimetric analysis (TGA) and differential scanning calorimetry (DSC) analysis [124]. With addition analysis of gas chromatography (GC) coupled with Fourier transform infrared spectroscopy (FTIR) by depolymerizing the PHA into acids, diols, or ester, the identified monomeric composition of PHA was usually correlated with its thermal properties [125]. FTIR analysis can provide more details about the chemical structure of PHA by detecting the functional groups of the PHA molecule. The presence of strong carbonyl marker bands in the 1700 cm^{-1} reveals the backbone of PHA chemical structure, where the carbonyl group's oxygen atoms being closer to hydrogen atoms,